BIOSYNTHESIS OF POLY ACRYLIC ACID (PAA) MODIFIED SILVER NANOPARTICLES, USING BASIL LEAF EXTRACT (*Ocimum basilicum L.*) FOR HEAVY METAL DETECTION

Yussi Pratiwi*, Yusmaniar, and Nurhasanah

Chemistry Program Study, Faculty of Mathematics and Natural Science, Universitas Negeri Jakarta, Indonesia

ARTICLE INFO	ABSTRACT
  	This study focused on characterizing synthesized silver nanoparticles (AgNPs) and evaluating their efficacy as colorimetric detectors for heavy metal ions. The synthesis employed a bottom-up approach, using $AgNO_3$ as a precursor, reduced by secondary metabolites in basil leaf extract, enhanced with Polyacrylic acid (PAA). Basil leaves were chosen for their rich content of secondary metabolites like phytosterols, alkaloids, phenolic compounds, tannins, lignin, starch, saponins, flavonoids, terpenoids, and anthraquinones, crucial in reducing silver ions. Incorporating basil leaf extract as a bioreactor and adding PAA to increase stability and selectivity towards metal ions are innovative aspects of this research. The optimal AgNP composition was attained with a 0.7 mL basil leaf extract to 10 mL $AgNO_3$ ratio plus 2% PAA. The AgNP formation was indicated by a color change from yellow to brownish, with a Surface Plasmon Resonance (SPR) peak at 418 nm. Characterization via Fourier Transform Infrared Spectroscopy (FTIR) revealed hydroxyl (-OH) and carbonyl (C=O) functional groups aiding in silver ion reduction. Particle Size Analysis (PSA) showed AgNPs of 72.3 nm size, with a polydispersity index of 0.504. Colorimetric detection tests were conducted on Cu(II), Pb(II), Cd(II), Zn(II), and Mn(II) ions. AgNPs exhibited high reactivity towards Cu^{2+}, changing color from brownish to clear white within a minute upon $Cu2+$ addition, unlike Cd^{2+}, Mn^{2+}, Zn^{2+}, and Pb^{2+}, which showed negligible changes. This indicates a heightened sensitivity of AgNPs to Cu^{2+} ions. Such a colorimetric sensor could be instrumental in detecting heavy metals in drinking water, showcasing the potential application of AgNPs in environmental monitoring.

INTRODUCTION

Environmental pollution by heavy metal contaminants has recently emerged as a formidable threat. This escalation is attributed to the excessive use of pesticides, rapid urbanization, and burgeoning industrial activities, leading to increased toxic metal ion contamination in ecosystems. The insidious nature of water pollution by heavy metals poses a significant risk to human health, given the propensity of these metals to bioaccumulate in the human body, potentially leading to various health disorders [1]. If unaddressed, the persistence of such pollution can evolve into a grave environmental hazard.

Heavy metals such as copper, nickel, arsenic, manganese, aluminum, and copper ions are known for their toxicity, inability to biodegrade, and tendency to accumulate in human and animal bodies [2].

Lead (Pb), in particular, is a toxicant known for its accumulation in human organs, leading to health issues such as anemia, renal impairment, and disorders affecting the nervous system, brain, and skin. Although certain heavy metals regulate human metabolism, their presence at elevated concentrations can have detrimental health effects, including hepatotoxicity, organ failure, and nephrotoxicity [3].

Given the health risks of heavy metals, there is a pressing need for sensitive and selective analytical methods for environmental detection. Silver nanoparticle-based sensors present a promising alternative to conventional detection methods such as Atomic Absorption Spectroscopy (AAS) and Inductively Coupled Plasma Mass Spectrometry (ICP-MS) [4]. Traditional methods like AAS and ICP-MS often require extensive preparation and processing time. In contrast, colorimetric sensors based on silver nanoparticles offer exceptional optical properties and straightforward synthesis advantages. Consequently, they are emerging as viable tools for the colorimetric detection of heavy metal ions in various samples, presenting a more accessible and efficient approach to environmental monitoring.

By their diminutive size, Nanoparticles exhibit superior optical, electronic, magnetic, and catalytic properties compared to their larger counterparts. Among these, the optical properties of silver nanoparticles (AgNPs) are particularly noteworthy due to their unique coloration due to their nanoscopic scale [5]. AgNPs are increasingly being recognized for their potential in biosensor development. In such applications, nanoparticles enhance biomolecule mobilization, catalyze electrochemical reactions, and facilitate electron transfer, making

them ideal for colorimetric detection of various metal samples [6].

The synthesis of silver nanoparticles can be approached via two primary methods: top-down (physical) and bottom-up (chemical). The top-down approach involves reducing large materials into nano-sized particles using mechanical, electrical, or thermal energy [7]. In contrast, the bottom-up method involves the addition of precursors, reducers, and stabilizers to synthesize nanoparticles.

Biosynthesis, a bottom-up approach, is gaining attention as a greener alternative to traditional chemical methods. This technique offers several advantages, including readily available natural materials, enhanced efficiency, cost-effectiveness, and environmental sustainability. Notably, the biosynthesis of silver nanoparticles leverages secondary metabolites, which facilitate the reduction of silver ions [8]. For instance, hydroxyl and carbonyl groups in basil leaf secondary metabolites can reduce Ag^+ to Ag^0, leading to the nucleation and formation of nano-sized Ag particles [9].

AgNPs are distinguished by their superior optical properties, including a higher extinction coefficient than other metal nanoparticles. This results in heightened visibility and sensitivity, enabling their application as colorimetric sensors for environmental pollutants like heavy metals. However, AgNPs can clump, affecting their size stability and sensory responsiveness. Thus, synthesis modification is crucial to enhance their selectivity and sensitivity as colorimetric sensors. Stabilizers in AgNP synthesis can control nanoparticle size and morphology, preventing aggregation and maintaining optimal size [10].

This study synthesized silver nanoparticles using basil leaf extract, modified with polyacrylic acid (PAA) as a stabilizer. Basil leaves were chosen for their rich secondary metabolite content, aiding in the silver ion reduction. PAA acts as a stabilizing agent, controlling nanoparticle size and morphology through surface energy reduction and providing steric effects for dispersion in suspension [11]. This modification aims to make AgNP-based sensors more sensitive and selective, particularly for certain analytes in environmental samples.

METHODS

1. Chemicals and Materials

Basil leaf extract (Ocimum basilicium L.) was air-dried in sunlight for ten days, $AgNO_3$, $Pb(NO_3)_2$, $3CdSO_4.8H_2O$, $ZnCl_2$, $CuCl_2.2H_2O$, $MnSO_4.H_2O$, magnesium metal, $FeCl_3$ solids, HCl, H_2SO_4, chloroform, anhydrous acetic acid, aquabidest, PAA, Dragendroff reagent, and Mayer reagent.

2. Extraction of Basil Leaf and Phytochemical Testing

Basil leaves are washed and then dried to remove their water content. The purpose of reducing water content is to avoid decay. After that, the leaves are pulverized using a blender until they become a homogeneous powder and filtered using a 60-mesh sieve. The purpose of pulverizing is to produce a fine powder size with a large surface area so that the contact of chemical additive molecules with the active compounds in the sample is faster. Then, as much as 3 grams of pureed basil leaves were boiled in an Erlenmeyer flask containing 200 mL of aquabides. The extract was filtered using Whatman No. 1 filter paper to take the filtrate.

The second filtration was done with a centrifugation at 3000 rpm for 15 minutes. The extract can be used immediately or stored at 4-8˚C. Furthermore, phytochemical tests were carried out to determine the class of compounds contained in basil leaf extract. In the synthesis of silver nanoparticles, the reduction and stabilization process of silver ions is due to the presence of important functional groups, including hydroxyl, carbonyl, amide, and carboxyl in secondary metabolite compounds such as ketones, terpenoids, flavonoids, aldehydes, steroids, alkaloids, tannins, saponins, and quinones in plant extracts. Phytochemical tests on basil leaf extract include alkaloid, flavonoid, terpenoid, steroid, and tannin tests.

There are 2 tests to determine the presence of alkaloid compounds in the sample: a sample of 2 mL plus 15 drops of concentrated H_2SO_4, then divided into 2 tubes; the first tube adds 5 drops of Dragendrof reagent (positive results from red to orange deposits), the second tube adds 5 drops of Mayer reagent (positive results form yellowish-white deposits) [12]. The flavonoid test is done by taking 1 mL of extract and heating it for 5 minutes, then adding 0.1 gram of Mg metal and 5 drops of concentrated HCl. If the solution forms an orange-yellow to red color, it is favorable to contain flavonoids [13]. The terpenoid and steroid tests are done by taking 1 mL of filtrate into 2 different test tubes and adding as much as 1 mL chloroform and 0.5 mL of anhydrous acetic acid. Then, 1 mL of concentrated H_2SO_4 was added to the mixture. Positive test results are characterized by forming a brownish ring on the border of the two solvents. In contrast, the positive results of the terpenoid test are marked by the formation of a blue-green color [14]. The tannin test takes as much as 1 mL of extract and then heated 5 minutes. Then, 3-5

drops of $FeCl_3$ 1% were added. If the solution forms a greenish-brown or blackish-blue color, it is positive for tannins [15].

3. Optimization of Silver Nanoparticle Synthesis

Basil leaf extract was mixed with 1 mM $AgNO_3$ solution with variations in the ratio of basil leaf extract: $AgNO_3$ (v/v), namely 0.5:10 (A), 0.7:10 (B), and 1:10 (C). The reason behind testing different ratios is to find the most optimum AgNPs produced because AgNPs themselves can indeed be synthesized with variations in several parameters to improve their capabilities. Then, the mixture was stirred until homogeneous using a magnetic stirrer and placed on a hot plate with a temperature of 80°C for 10 minutes. Meanwhile, with higher temperatures, the size of silver nanoparticles formed is smaller. This is because, at this temperature, some of the stabilizing compounds are damaged. After that, 2 mL of PAA solution (1%, 2%, and 3%) was added dropwise until a brownish-yellow color was obtained without heating. Then, the colloidal silver nanoparticles formed until the 30th day after synthesis were observed, and the absorbance was measured with a UV-Vis spectrophotometer. Furthermore, the synthesis process was repeated without using a PAA stabilizer solution as a comparison to find out how stable AgNPs are without using a stabilizer. The sample code of the synthesized silver nanoparticles can be seen in Table 1.

Table 1. Code of the sample AgNP

Volume ratio (mL)	Concentration PAA		
Extract: $AgNO_3$	1%	2%	3%
0,5 : 10	KA1	KA2	KA3
0,7: 10	KB1	KB2	KB3
1 : 10	KC1	KC2	KC3

4. Characterization of Silver Nanoparticles

The resulting silver nanoparticles were then characterized with a UV-Vis spectrophotometer to determine whether the synthesized nanoparticles had entered the nanoparticle size range by looking at the absorbance and wavelength produced. The absorption peak of silver nanoparticles has strong absorption at wavelengths between 400–500 nm [16]. Then, characterization was carried out with FTIR to determine the bonding of functional groups that act as bioreactors in the synthesis of AgNP, and the group was characterized with PSA to obtain the average particle size distribution. Particle size data is obtained in the form of three distributions, namely intensity, number, and volume distribution, so it can be assumed to describe the overall condition of AgNP [17].

5. Colorimetric Analysis Based on Silver Nanoparticles

Each analyte solution containing Cd^{2+}, Cu^{2+}, Pb^{2+}, Mn^{2+}, and Zn^{2+} ions was pipetted as much as 1 mL with a concentration of 1000 ppm and then added 2 mL of silver nanoparticles. Furthermore, it was observed visually, and the time of each solution's color change was recorded. Metal analytes that experience color changes become clear, indicating that the metal ions are most sensitive to AgNP. If a high concentration of color change occurs, then the analysis is continued with a lower concentration of 0.1, 1, 10, 100, 500, and 1000 ppm. The analysis is to determine the limit sensitivity testing of the ability of AgNPs to detect selected metal ions spectrophotometrically.

RESULTS AND DISCUSSION

1. Extraction of Basil Leaf and Phytochemical Testing

The commencement of this research involved the preparation of basil leaf extract. The extraction process yielded 125 mL of basil leaf filtrate from an initial volume of 200 mL, aligning with expectations as minimal water was lost. Low yields in the extraction phase could impact the subsequent synthesis of silver nanoparticles (AgNPs).

Table 2. Code of the sample AgNP

Class of Secondary Metabolites	Result	Remarks
Alkaloid (Dragendroff)	+	Brownish red precipitate
Alkaloid (Meyer)	+	Brownish white precipitate
Flavonoid	+	Yellow solution with lots of brownish-yellow foam
Terpenoid	+	Brownish ring
Steroid	-	No change
Tanin	+	Blackish green color

Following the extraction, phytochemical tests were conducted to qualitatively assess the presence of secondary metabolite compounds in the basil leaf extract. These compounds' specific functional groups act as bioreductors in the AgNP synthesis. The phytochemical analysis entailed the addition of specific reagents to the extract, inducing characteristic color changes. These changes serve as indicators of various secondary metabolite compound groups present in the basil leaf extract.

The outcomes of this phytochemical screening, detailing the identified secondary metabolite content in basil leaves, are presented in Table 2. Identifying these compounds is crucial, as they play a pivotal role in the reduction process that leads to forming

AgNPs. Understanding the composition and concentration of these metabolites aids in optimizing the synthesis process and enhances the resulting nanoparticles' efficacy.

Table 2 illustrates the results of the phytochemical testing conducted on basil leaves. The analysis revealed the presence of various secondary metabolites, including alkaloids, flavonoids, terpenoids, and tannins. However, the test results were negative for steroids. These findings are consistent with other studies that have analyzed basil leaves, where positive results were obtained for phenolics, alkaloids, tannins, saponins, flavonoids, terpenoids, and anthraquinones [18]. In this study, the absence of steroids was confirmed by the negative outcome in the steroid-specific test among the five tests conducted.

Secondary metabolite compounds, particularly those with hydroxyl (-OH) and carbonyl (-CO) groups, are significant as these functional groups can bind to metal ions. They donate electrons to Ag+ ions, facilitating the reduction to Ag0. This electron donation process is crucial in synthesizing silver nanoparticles, where these functional groups effectively contribute to reducing silver ions.

Thus, rich in these secondary metabolites, the basil leaf extract demonstrates considerable potential as a bioreductor in synthesizing silver nanoparticles [19]. The presence of these specific functional groups in the extract underscores its suitability for use in the biosynthesis of silver nanoparticles, making it an effective and environmentally friendly alternative to conventional chemical reduction methods.

2. Optimization of Silver Nanoparticle Synthesis

The subsequent phase of this research was devoted to optimizing the synthesis of silver nanoparticles (AgNPs) to establish the most favorable conditions for producing optimal nanoparticles. This optimization involved varying parameters, including the volume of basil leaf extract, the concentration of Polyacrylic acid (PAA) stabilizer, and the storage duration of the nanoparticles, to assess their stability.

The initial step entailed determining the optimal volume ratio of basil leaf extract to 1 mM $AgNO_3$ precursor solution in AgNP synthesis. Three different volume ratios of basil leaf extract to $AgNO_3$ (v/v) were tested: 0.5:10 (A), 0.7:10 (B), and 1:10 (C). Each of these variations was further experimented with three different concentrations of PAA stabilizer solution: 1%, 2%, and 3%, as shown in Figure 1. A parallel synthesis was conducted without the stabilizer solution for comparative purposes.

Figure 1. AgNP colloidal sample.

Typically, the formation of colloidal silver nanoparticles manifests as a progressive color change in the solution from colorless to yellow, eventually turning brownish. Initially, upon mixing the $AgNO_3$ solution with basil leaf extract, the solution exhibited a pale yellow color. After 30 minutes of stirring, the solution transitioned to a bright yellow shade and gradually darkened to brownish. This observable color transition also signifies

alterations in the optical properties of the nanoparticles.

UV-Visible (UV-Vis) spectrophotometry was employed to corroborate the formation of AgNPs quantitatively. The Surface Plasmon Resonance (SPR) values of AgNPs characteristically peak within the λmax range of 400-500 nm. The UV-Vis spectra indicated new absorption peaks in the 435-445 nm region, confirming the biosynthesis of AgNPs. Additionally, an increase in absorbance values was noted, along with a sharpening of the characteristic peak width over time. This trend suggests increased quantity and homogeneity of the AgNPs formed.

a. Effect of Volume of Basil Leaf Extract

The experimental observations revealed that the volume ratios of basil leaf extract to $AgNO_3$, specifically 0.5:10 (KA), 0.7:10 (KB), and 1:10 (KC), exhibited distinct absorbance peaks at 24 hours following the synthesis process. The peak wavelengths were recorded at 445 nm for KA, 439 nm for KB, and 441 nm for KC. These findings align with the anticipated formation of silver nanoparticles (AgNPs). In comparison, a study involving the synthesis of AgNPs using watermelon leaf extract reported an absorbance spectrum range of 440–446 nm [19], congruent with the wavelength range observed in this study for AgNPs synthesized using basil leaf extract.

The UV-visible optical absorption spectra, particularly the peak wavelength values of the synthesized AgNPs, are determined by nanoparticle size, shape, and the dielectric properties of the surrounding medium. These spectra result from the Localized Surface Plasmon Resonance (LSPR) phenomenon, characterized by the collective electron oscillations in

specific vibrational modes within the conduction band near the nanoparticle surface. The LSPR responds to electromagnetic radiation, causing electron vibrations in the conduction band adjacent to the AgNP surface.

Analyzing the absorbance values, the 1:10 (KC) variation displayed the highest absorbance, suggesting a higher concentration of AgNPs compared to the 0.5:10 (KA) and 0.7:10 (KB) variations. This implies a correlation between absorbance intensity and AgNP quantity, where a higher absorbance indicates greater AgNP synthesis [20]. These findings demonstrate that an increase in the volume of basil leaf extract correlates with enhanced AgNP production. Thus, basil leaf extract is efficacious as a bioreductor in synthesizing AgNPs across all evaluated variations. However, to ascertain the optimal ratio for efficient AgNP synthesis, further analysis is warranted, particularly focusing on varying concentrations of the PAA stabilizer, ranging from 1% to 3%.

b.   Effect of PAA Stabilizer Concentration

After 24 hours, the AgNPs modified with 1%, 2%, and 3% Polyacrylic acid (PAA) exhibited a trend of wavelength shift towards shorter wavelengths, accompanied by a decrease in absorbance. Notably, AgNP samples with 3% PAA addition demonstrated a significantly smaller wavelength shift than those with 1% and 2% PAA. This suggests that higher concentrations of PAA stabilizers can effectively mitigate the rate of nanoparticle agglomeration, as indicated by the shift in wavelength towards shorter values, reflective of changes in particle size. As the PAA concentration increases, the particle size distribution becomes narrower, and the particle sizes formed are smaller.

The concentration of PAA influences the morphology of AgNP crystals predominantly through steric effects. PAA forms shorter chains at lower concentrations, reducing steric hindrance and effective interaction with AgNPs in colloidal solutions. However, this concentration might be less effective in preventing nanoparticle agglomeration. Conversely, higher PAA concentrations lead to the formation of longer PAA chains, which provide better protection against AgNP agglomeration. This steric hindrance becomes critical in inhibiting agglomeration as the nanoparticles begin to grow [21]. Modifying AgNPs with 3% PAA has enhanced nanoparticle stability, maintaining the size of AgNPs more effectively.

The interaction between PAA molecules and metal atoms on the nanocrystal surface occurs through the affinity of oxygen and nitrogen donor atoms present in the carbonyl amide groups of PAA. These interactions lower the surface energy, inhibiting grain growth and particle agglomeration [22]. This mechanism highlights the role of PAA in stabilizing the AgNPs and dictating their size and distribution, which is essential for the effective application of these nanoparticles in various fields.

c.   Stability of Silver Nanoparticles

The stability of synthesized silver nanoparticles (AgNPs) was evaluated through UV-visible spectrophotometry over 30 days at room temperature. The AgNPs, synthesized using basil leaf extract, displayed a shift in their maximum wavelength. This wavelength remained within the characteristic AgNP range of 435–440 nm, and an increase in absorbance was observed over the duration [19]. This trend is consistent with observations noted in other

studies, where similar spectral shifts were documented over extended storage periods [20].

The shift in maximum wavelength and the rise in absorbance suggest an increase in particle size over time, likely due to nanoparticle agglomeration. This phenomenon is further influenced by the bathochromic effect, a result of specific substituents in the chromophores of the basil leaf extract's secondary metabolite compounds. Additionally, the increase in absorbance over time indicates ongoing AgNP formation, a process known as the hyperchromic effect.

When analyzing all sample variations, it was observed that the particle size distribution in the sample with 0.7 mL basil leaf extract and 2% PAA (KB2) exhibited increasing homogeneity. Consequently, the synthesized AgNPs demonstrate adequate stability for up to 30 days, making them viable for use as colorimetric sensors [21]. However, further analysis utilizing Particle Size Analysis (PSA) is recom-

mended to confirm particle size distribution accurately. The KB2 sample showed the most robust stability among all variations during the 30-day storage period, indicating that the synthesis ratio used in this sample is optimal for further nanoparticle synthesis, particularly for applications in colorimetric sensing [22].

3. Characterization of Silver Nanoparticles

Characterization is a crucial stage to determine the size, shape, morphology, structure, surface chemistry, surface charge, dispersion, and surface area of the nanoparticles that have been synthesized.

a. Characterization with FTIR

The characterized samples were selected based on the most optimum formulation: AgNPs synthesized from 0.7 ml of basil leaf extract and 2% PAA solution. The FTIR spectra of the synthesized nanoparticle samples can be seen in Figure 2.
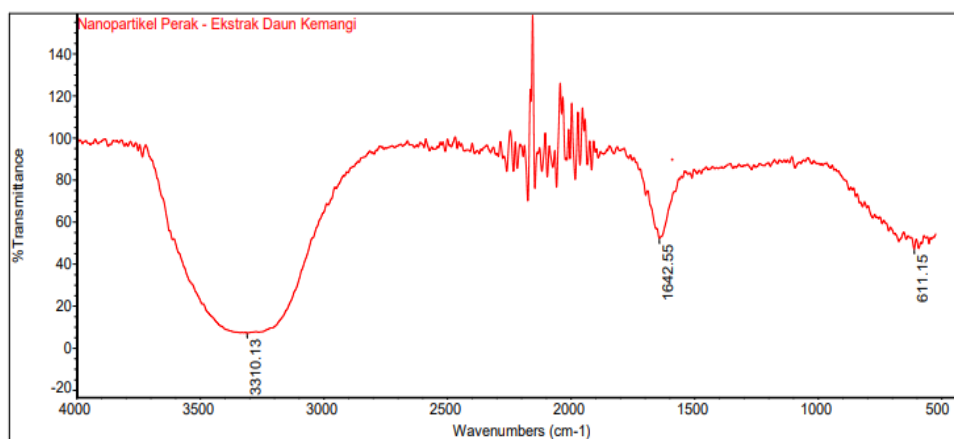

Figure 2. FTIR spectra of AgNP.

The Fourier Transform Infrared Spectroscopy (FTIR) analysis of the synthesized silver nanoparticles (AgNPs) revealed characteristic absorption bands. An absorption band at a wavenumber of 3310.13 cm^{-1} indicates O-H stretching, suggesting the presence of hydroxyl

groups in compounds such as alcohols, phenolics, and flavonoids. Similar findings were reported [23], where FTIR spectra at wavenumbers 3386.14 cm^{-1} and 3393.69 cm^{-1} indicated OH groups from hydrogen bonds. Absorption bands at 1637.22 cm^{-1} and 1637.37

cm^{-1} correspond to C=C (alkene) groups, while bands at 1399.47 cm^{-1} and 1355.14 cm^{-1} denote -CH$_3$ groups. Bands at 1217.41 cm^{-1} and 1217.22 cm^{-1} suggest the presence of C-O groups.

Peaks in the range of 3000-3500 cm^{-1} indicate stretching vibrations of hydroxyl (-OH) or amine (-NH$_2$) groups, associated with phenols and flavonoids, and bands at 1600-1690 cm^{-1} are indicative of phenols and flavonoids, leading to carbonyl groups (C=O). These could also indicate amine groups (-NH$_2$) from PAA molecules in AgNPs. An absorption band at 1642.55   cm^{-1} corresponds to C=O stretching, which is characteristic of carbonyl groups, and a band at 611.15 cm^{-1} represents C=C ring stretching vibrations or AgNP stretching vibrations.

As reported [24], bands in 1400-1600, 1640-1690, 2850-3500, and 1000-1300 cm^{-1} are associated with reducing silver nanoparticles. FTIR analysis confirms the presence of hydroxyl (-OH), amine (-NH$_2$), and carbonyl (-C=O) groups as functional groups responsible for reducing Ag$^+$ ions to Ag^0. Comparisons between the IR spectra of plant extracts before and after reaction with Ag$^+$ ions revealed minimal changes, except for a slight decrease in peak intensity of functional groups, as detailed in Figure 3. This suggests the mechanism of interaction between functional groups in basil leaf extract and Ag$^+$ ions.
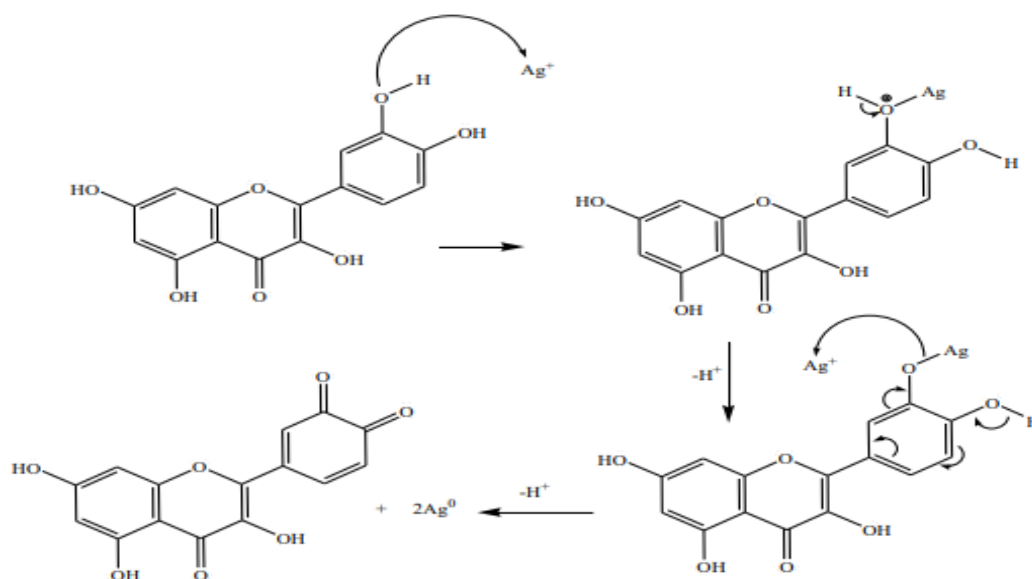
Figure 3. Reaction Mechanism of AgNP   Formation.

It was reported that the bands in the wave number range of 1400-1600, 1640-1690, 2850-3500, and 1000-1300 cm^{-1} are the groups that assist in reducing silver nanoparticles. FTIR analysis confirmed hydroxyl (-OH), amine (-NH$_2$), and carbonyl (-C=O) groups as the functional groups responsible for the reduction of Ag$^+$ ions to Ag^0. The results between the IR spectra of plant extracts, before they reacted with Ag$^+$ ions and after silver nanoparticles were formed, did not provide significant changes but only a slight decrease in the peak intensity of functional groups. Thus, the alleged mechanism between the functional groups in the compounds in basil leaf extract and Ag$^+$ ions is presented explicitly in Figure 3.The biosynthesis of silver nanoparticles (AgNPs) using plant extract bioreductors primarily involves the reduction of Ag$^+$ ions to Ag^0. Secondary metabolites in plants, rich in func-

tional groups such as hydroxyl, carboxylate, and carbonyl, exhibit a pronounced affinity for forming bonds with metal ions. These functional groups interact with Ag^+ ions, leading to the formation of intermediate complexes. Ag particles exhibit mutual repulsion due to like charges in their ionic form. However, upon reduction to Ag^0, the charge on the Ag atoms is neutralized, thereby facilitating the aggregation of Ag atoms—this aggregation, driven by inter-metallic bonding, results in the formation of nano-sized clusters.

During this biosynthetic process, the functional groups within the plant extracts undergo oxidation reactions, leading to transformations such as the conversion of hydroxyl groups (-OH) into ketone groups. This alteration in functional groups decreases their quantity within the sample following the oxidation reactions. Consequently, the synthesis of AgNPs, due to the reduction of Ag^+ ions by plant extracts, can be inferred from the observed reduction in the peak intensity of functional groups in the plant extracts' infrared (IR) spectra. This decrease in peak intensity is noted when comparing the IR spectra before and after the reaction with Ag^+ ions and subset the sent formation of AgNPs. Such changes in the IR spectra indicate the successful biosynthesis of silver nanoparticles by reducing Ag^+ ions using plant-based bioreductor.
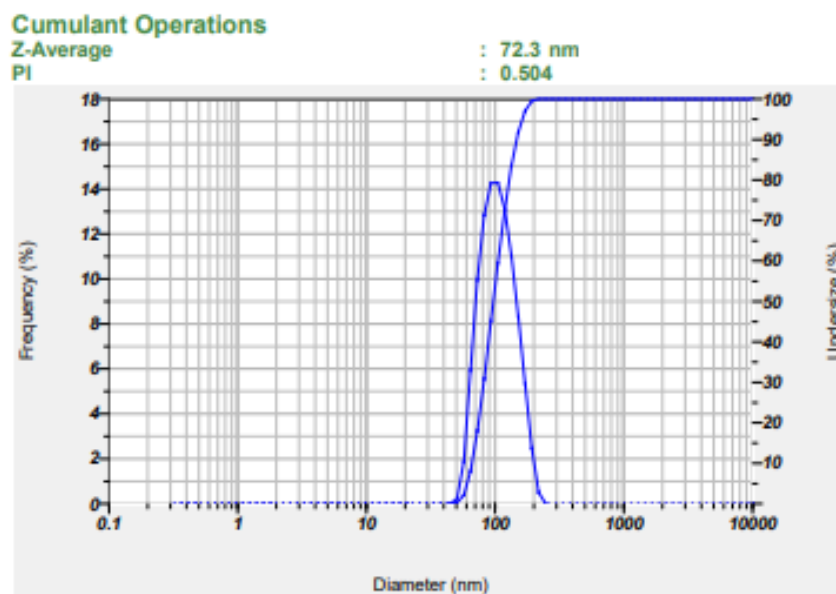
b. Characterization with PSA

Characterization via Particle Size Analyzer (PSA) is instrumental in determining the size distribution of synthesized nanoparticles. This characterization is crucial in confirming the suitability of the synthesized AgNPs for application as heavy metal colorimetric sensors. The samples were deemed optimal, specifically synthesized using a formulation of 0.7 ml basil leaf extract and a 2% PAA solution.

As depicted in Figure 4, the PSA results revealed that the AgNPs synthesized using basil leaf extract achieved a particle size of 72.3 nm. This size aligns with the general definition of nanoparticles, classified as materials with dimensions ranging from 1–100 nm. Furthermore, the use of a PAA stabilizer in this study successfully maintained the AgNP size below 80 nm for up to 7 days, signifying good stability of the sample. These findings corroborate the relationship between the maximum wavelength (λmax) and the size of silver nanoparticles; the AgNPs with a λmax of 438 nm correspond to a size within the 60–80 nm. Therefore, it can be concluded that the AgNPs produced under these optimum conditions fall within the nanoparticle size category.

The characterization outcomes from the PSA affirm that the AgNPs synthesized under optimal conditions indeed qualify as nanoparticles. This categorization is crucial for their intended use in colorimetric sensing applications, where nanoparticle size can significantly influence sensor performance and sensitivity. The Particle Size Analyzer (PSA) results also indicated a Polydispersity Index (PDI) value of 0.504 for the synthesized silver nanoparticles (AgNPs). This value suggests that the AgNP sample exhibits polydispersive properties with a relatively uniform size distribution. Generally, a lower PDI value implies a narrower nanoparticle size distribution, indicating greater homogeneity (monodispersity) in the nanoparticle diameter sizes. The PDI scale ranges from 0 to 1, where values close to 0 denote a homogeneous dispersion and a PDI value greater than 0.5 indicates a high degree of heterogeneity.

Figure 4. PSA test result.

The PSA characterization demonstrates that using basil leaf extract bioreductors and adding a Polyacrylic acid (PAA) stabilizer effectively reduces the agglomeration of silver nanoparticles, resulting in smaller AgNP sizes. Moreover, the graph depicting the PSA results forms a single peak, which indicates good uniformity in the sample and no significant increase in particle size [23]. This single-peak profile strongly indicates that the sample does not undergo aggregation, which would otherwise lead to an increase in particle size.

These findings underscore that incorporating a PAA stabilizer is important in controlling the microstructure and Localized Surface Plasmon Resonance (LSPR) properties of AgNP biosynthesis. The ability of PAA to prevent nanoparticle aggregation and maintain a uniform size distribution enhances the potential of these biosynthesized AgNPs as effective components in future LSPR-based sensors. The controlled microstructure and optimized LSPR characteristics of AgNPs are crucial for their application in sensitive and precise sensing technologie

c. Colorimetric Analysis

Qualitative colorimetric and spectroscopic analyses were conducted to assess the selectivity of the synthesized silver nanoparticles (AgNPs) towards heavy metal ions. The fundamental mechanism of AgNP-based colorimetric sensing relies on the aggregation of nanoparticles upon interaction with analytes. This aggregation leads to a Localized Surface Plasmon Resonance (LSPR) shift towards higher wavelengths. LSPR is a phenomenon where silver nanoparticles absorb and scatter light at specific wavelengths, and this aggregation increases in particle size, accompanied by a characteristic color change [24]. Therefore, AgNPs can serve as effective sensors for detecting various analytes, including heavy metal ions.

The results of the colorimetric tests are presented in Table 3 and illustrated in Figure 5. These results demonstrate the potential of AgNPs as a colorimetric tool for the selective detection of heavy metal ions. The observed color change, a direct consequence of the LSPR shift, indicates the presence and concentration of specific heavy metal ions in the

tested samples. This property of AgNPs makes them particularly useful in environmental monitoring and analysis, where rapid and accurate detection of heavy metal ions is crucial. The ability of AgNPs to provide visual and spectroscopic evidence of ion aggregation makes them a valuable asset in developing efficient and user-friendly sensing technologies.

Table 3. Colorimetric Test Results

| Metal Ions	Result
Cd^{2+}	Brown → Light brown (-)
Mn^{2+}	Brown → Light brown (-)
Pb^{2+}	Brown → Light brown (-)
Zn^{2+}	Brown → Orange (-)
Cu^{2+}	Brown → light green(+)

Remarks:
(+) Result: No 400-500 nm peak shows that the silver nanoparticles have grouped and moved out of their usual range.
(-) Result: A 400-500 nm peak is seen, but it could be stronger in the original solution. This suggests minor grouping and the nanoparticles are still mostly in their normal range. The color looks a bit less intense.

This change can occur due to AgNP aggregation when in contact with the analyte, which will interfere with the interaction of the Ag^0 dipole-ion with oxygen/nitrogen in the PAA molecule [25], so the stability of AgNP is reduced and tends to experience aggregation. When viewed from the cell potential price (E0), Cu^{2+} ions have an E^0 price of +0.34. This value is more significant than Cd^{2+}, Mn^{2+}, Zn^{2+}, and Pb^{2+} metals, which have E^0 prices of -0.4, -1.185, -0.762, -0.13, respectively, thus causing Cu^{2+} ions to be more easily reduced by Ag^0 than other metal ions.

Figure 5 illustrates the colorimetric response of silver nanoparticles (AgNPs) to various metal ions, highlighting Cu^{2+} as the ion to which AgNPs are most sensitive. This sensitivity is evidenced by the immediate color change from the original brownish-yellow hue of

AgNPs to light green upon interaction with the Cu^{2+} analyte. In contrast, tests conducted with Zn^{2+}, Pb^{2+}, Cd^{2+}, and Mn^{2+} ions did not exhibit any significant color changes, indicating a specific sensitivity of AgNPs towards Cu^{2+} ions. This color transformation results from the aggregation of AgNPs triggered by the analyte, leading to reduced stability and subsequent aggregation.
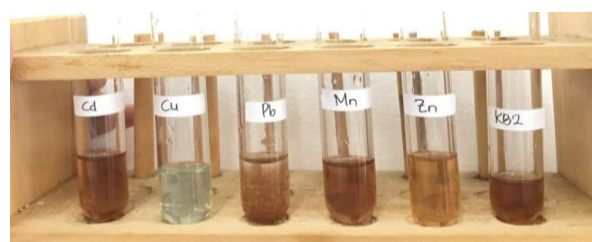
Figure 5. Colorimetric test result.

Figure 6. Colorimetric Test of Various Concentrations of Cu^{2+} Ion.

The interaction between Polyacrylic acid (PAA) and Cu^{2+} ions contributes not only to AgNP aggregation but also influences the electronic structure of PAA, manifesting in the observable Localized Surface Plasmon Resonance (LSPR) effect. PAA serves dual roles in this context - as a stabilizer and as an ion coordination reagent. PAA's nitrogen and oxygen atoms can form specific coordination complexes with Cu^{2+} ions [26].

According to UV-visible spectroscopy data, the absorbance of AgNPs is no longer detectable in samples mixed with Cu^{2+} metal, signifying an alteration in the characteristic properties of AgNPs. Conversely, the spectra for Zn^{2+}, Pb^{2+}, Cd^{2+}, and Mn^{2+} tests maintained typical AgNP absorbance, with peaks in the

400–500 nm wavelength range. Therefore, additional tests with lower concentrations of Cu^{2+} ions were conducted to analyze the absorbance characteristics more precisely.

Subsequent testing on varying concentrations of Cu^{2+} ions, from 1000 ppm to 0.1 ppm (Figure 6), qualitatively showed significant colloidal color changes from 1000 ppm to 100 ppm. In contrast, tests with Cu^{2+} concentrations from 10 ppm to 0.1 ppm exhibited less pronounced changes. The UV-Vis spectral analysis revealed decreased absorbance values across all Cu^{2+} ion concentrations and a shift in wavelength towards longer wavelengths. This indicates reduced electrostatic repulsion and accelerated agglomeration. Such agglomeration brings the AgNPs closer together, weakening the ion-dipole interaction between the AgNPs and P.

As the amount of AgNP increases, the ability of Cu^{2+} ions to interfere with the dipole-ion interaction of $Ag0$ with PAA decreases. Therefore, the influence of low concentrations of analytes relatively does not interfere with the stability of AgNP, and less agglomeration occurs. The results of this test conclude that the smaller concentration of Cu^{2+} analyte added causes the color change to occur longer because changes in concentration are related to the reaction rate.

CONCLUSION

Based on the comprehensive data analysis encompassing the impact of basil extract addition, the influence of Polyacrylic acid (PAA), storage time stability, and the visual characteristics of the AgNP colloids, the KB2 sample was selected for the colorimetric testing. This sample demonstrated optimum characteristics, comprising AgNPs with an $AgNO_3$ to basil extract ratio of 0.7:10 and a 2% PAA addition. The synthesized nanoparticles exhibited an average particle size of 72.3 nm, a maximum absorption peak at a wavelength of 418 nm, and a homogeneous dispersion profile. The silver nanoparticles showed a high selectivity towards Cu^{2+} ions, as evidenced by the color transition from brownish to clear white. This change was accompanied by a spectral shift towards longer wavelengths, indicative of nanoparticle aggregation. The sensitivity of the AgNPs to Cu^{2+} ions was highlighted by their response to a concentration as low as 0.08 mg L^{-1}. For future research directions, it is recommended to optimize additional parameters such as pH and temperature to enhance the selectivity of AgNPs towards other heavy metals, including mercury (Hg), arsenic (As), and lead (Pb). Further characterization of AgNPs using transmission electron microscopy (TEM) is suggested to determine the size distribution more accurately. Additionally, it would be beneficial to conduct tests with actual environmental samples to evaluate the practical applicability of these AgNPs in real-world scenarios. These steps will contribute significantly to advancing the field of heavy metal detection and environmental monitoring.

REFERENCES

[1]   D. S. Vijaykumar, T. Anbalagan ,M. Nithyanandan & N. Namboothri, "Watering Pot Shell, Brechites penis (Linnaeus, 1758), a new record to India (Mollusca: Bivalvia: Anomalodesmata)," *Journal of Threatened Taxa*, vol. 5, no. 12, pp. 4679–4681, 2013, doi: 10.11609/JoTT.o3479.4679-81.

[2]   J. Li, X. Wang, G. Zhao et al., "Metal–organic framework-based materials: superior adsorbents for the capture of

toxic and radioactive metal ions," *Chemical Society Reviews*, vol. 4, no. 7, pp. 2322–2356, 2018, doi: 10.1039/C7CS00543A.

[3] F. E .P, Almaquer & J.V.D, Perez, "Evaluation of the Colorimetric Performance of Unmodified Citrate-Stabilized Silver Nanoparticles for Copper (II) Sensing in Water," *Key Engineering Materials*, vol. 821, pp. 372–378, 2019, doi: 10.4028/www.scientific.net/kem.821.372

[4] M. Nurfadhilah, I. Nolia, W. Handayani & C. Imawan, "The Role of pH in Controlling Size and Distribution of Silver Nanoparticles using Biosynthesis from *Diospyros discolor Willd.* (Ebenaceae)," *IOP Conference Series: Materials Science and Engineering*, vol. 367, pp. 1-2, 2018, doi: 10.1088/1757-899X/367/1/012033.

[5] S. A. Akintelu, Y. Bo & A .S. Folorunso, "Review on Synthesis, Optimization, Mechanism, Characterization, and Antibacterial Application of Silver Nanoparticles Synthesized from Plants," *Journal of Chemistry*, vol. 2020, pp. 1–12, 2020, doi: 10.1155/2020/3189043.

[6] Z. Zhang, H. Wang, Z. Chen et al., "Plasmonic colorimetric sensors based on etching and growth of noble metal nanoparticles: Strategies and applications," *Biosensors and Bioelectronics*, vol. 114, pp. 52–65, 2018, doi: 10.1016/j.bios.2018.05.015.

[7] K. M. M. A. El-Nour, A. Eftaiha, A. Al-Warthan & R. A. A. Ammar, "Synthesis and applications of silver nanoparticles," *Arabian Journal of Chemistry*, vol. 3, no. 3, pp. 135–140, 2010, doi: 10.1016/j.arabjc.2010.04.008.

[8] D. Kalpana, J. H. Han, W. S. Park et al., "Green biosynthesis of silver nanoparticles using Torreya nucifera and their antibacterial activity," *Arabian Journal of Chemistry*, vol. 12, no. 7, pp. 1722–1732, 2019, doi: 10.1016/j.arabjc.2014.08.016.

[9] G. G. Michel, R. F. Sigal, F.. Civan & D.. Devegowda, "Parametric Investigation of Shale Gas Production Considering Nano-Scale Pore Size Distribution, Formation Factor, and Non-Darcy Flow Mechanisms," *SPE Annual Technical Conference and Exhibition*, Denver, Colorado, USA, October 2011, doi: 10.2118/147438-MS.

[10] T. Wahyudi, D. Sugiyana & Q. Helmy, "Synthesis of silver Nanoparticel and Acrivity Test against *E.coli* and *S. aureus* Bacteria," *Textile Arena*, vol. 26, no.1, pp. 55-60, 2011, doi: 10.31266/at.v26i1.1442.

[11] M. Nidya, M. Umadevi & B. J. M. Rajkumar, "Structural, morphological and optical studies of l-cysteine modified silver nanoparticles and its application as a probe for the selective colorimetric detection of Hg^{2+}," *Spectrochimica Acta - Part A: Molecular and Biomolecular Spectroscopy*, vol. 133, pp. 265–271. 2014, doi: 10.1016/j.saa.2014.04.193.

[12] T. Harningsih & W.Wimpy, "Uji Aktivitas Antioksidan Kombinasi Ekstrak Daun Kersen (*Muntingia calabura Linn.*) dan Daun Sirsak (*Anonna muricata Linn.*) Metode DPPH (2,2-diphenyl-1-picrilhidrazyl)," *Biomedika*, vol. 11, no. 2, pp. 70–75. 2018, doi: 10.31001/biomedika.v11i2.422.

[13] K. Mustikasari & D. Ariyani, "Skrining fitokimia ekstrak metanol biji Kalangkala (*Litsea angulata*)," *Sains dan Terapan Kimia*, vol. 4, no. 2, pp.131-136, 2010, doi: 10.20527/jstk.v4i2.2057.

[14] S. Kursia, J. S. Lebang & Nursamsiar "Uji Aktivitas Antibakteri Ekstrak Etilasetat Daun Sirih Hijau (*Piper betle L.*) terhadap Bakteri *Staphylococcus epidermidis*," *Indonesian Journal of Pharmaceutical Science and Technology*, vol. 3, no. 2, pp. 72–77, 2016.

[15] M. Marlinda, M. S. Sangi & A. D. Wuntu, "Analisis Senyawa Metabolit Sekunder dan Uji Toksisitas Ekstrak Etanol Biji Buah Alpukat (*Persea americana Mill.*)," *Jurnal MIPA*, vol. 1, no. 1, pp. 24-28, 2012, doi: 10.35799/jm.1.1.2012.427.

[16] L. Mulfinger, S. D. Solomon, M. Bahadory et al., "Synthesis and Study of

Silver Nanoparticles," *Journal of Chemical Education*, vol. 84, no. 2, p. 322, 2007,
doi: 10.1021/ed084p322.

[17]   S. Dawadi, S. Katuwal, A. Gupta et al., "Current Research on Silver Nanoparticles: Synthesis, Characterization, and Applications," *Journal of Nanomaterials*, vol. 2021, pp. 1–23., 2021,
doi: 10.1155/2021/6687290.

[18]   M. O. Ullah, M. Haque, K. F. Urmi et al., "Anti-bacterial activity and brine shrimp lethality bioassay of methanolic extracts of fourteen different edible vegetables from Bangladesh," *Asian Pac J Trop Biomed.,* vol. 3, no. 1, pp. 1-7, 2013,
doi: 10.1016/S2221-1691(13)60015-5.

[19]   N. Adrianto, A. M. Panre, N. I. Istiqomah et al., "Localized surface plasmon resonance properties of green synthesized silver nanoparticles," *Nano-Structures & Nano-Objects*, vol. 31. 2020,
doi: 10.1016/j.nanoso.2022.100895.

[20]   P. Singh, Y. Kim, D. Zhang & D. Yang, "Biological Synthesis of Nanoparticles from Plants and Microorganisms," *Trends in Biotechnology*, vol. 34, no. 7, pp. 588–599. 2016,
doi: 10.1016/j.tibtech.2016.02.006.[21]   Y. J. Song, M. Wang, X. Y. Zhang et al., "Investigation on the role of the molecular weight of polyvinyl pyrrolidone in the shape control of high-yield silver nanospheres and nanowires," *Nanoscale Research Letters*, vol. 9, no. 1, p. 17, 2014,

doi: 10.1186/1556-276X-9-17.

[22]   P. Sharma, S. Pant, S. Rai et al., "Green Synthesis of Silver Nanoparticle Capped with *Allium cepa* and Their Catalytic Reduction of Textile Dyes: An Ecofriendly Approach," *Journal of Polymers and the Environment*, vol. 26, no. 5, pp. 1795–1803, 2018,
doi: 10.1007/s10924-017-1081-7.

[23]   M. Nidhin, R. Indumathy, K. J. Sreeram & B. U. Nair, "Synthesis of iron oxide nanoparticles of narrow size distribution on polysaccharide templates," *Bulletin of Materials Science*, vol. 31, no. 1, pp. 93–96, 2008,
doi: 10.1007/s12034-008-0016-2.

[24]   J. V. Rohit, J. N. Solanki & S. K. Kailasa, "Surface modification of silver nanoparticles with dopamine dithiocarbamate for selective colorimetric sensing of mancozeb in environmental samples," *Sensors and Actuators B: Chemical*, vol. 200, pp. 219–226, 2014,
doi: 10.1016/j.snb.2014.04.043.

[25]   D. Xiong & H. Li, "Colorimetric detection of pesticides based on calixarene modified silver nanoparticles in water," *Nanotechnology*, vol. 19, no. 46, 2008,
doi: 10.1088/0957-4484/19/46/465502.

[26]   S. Maiti, G. Barman & J. K. Laha, "Detection of heavy metals (Cu^{+2}, Hg^{+2}) by biosynthesized silver nanoparticles," *Applied Nanoscience*, vol. 6, no. 4, pp. 529–538, 2016,
doi: 10.1007/s13204-015-0452-4.